# EFFECT OF SNOW WETNESS TO C-BAND BACKSCATTER - A MODELING APPROACH

*Jarkko Koskinen[1], Jouni Pulliainen and Martti Hallikainen*
*Helsinki University of Technology (HUT), Laboratory of Space Technology*
*P.O. Box 3000, FIN-02015 HUT, FINLAND.*

[1] *Currently with Finnish Environment Institute (FEI), GIS and Remote Sensing Group, P.O. Box 140, FIN-00250, Helsinki, FINLAND.*

# TABLE OF CONTENTS

# ABSTRACT

*A simple backscattering model is presented and its application to radar remote sensing of snow is discussed. Our snow model consists of three parts, (a) IEM surface scattering model for snow surface scattering, (b) a discrete scatterer volume scattering model and (c) the Michigan empirical surface scattering model for soil backscattering. Together with the snow-covered terrain backscattering model we use the HUT boreal forest semi-empirical backscattering model in order to analyze the effect of forest canopy for snow monitoring. The modeling results are compared with HUTSCAT airborne scatterometer and ERS-1 SAR data obtained during the winters of 1992 (wet snow conditions) and 1993 (dry snow conditions) in the Sodankylä test site in northern Finland. The model predictions agree with the experimental data even in the presence of forest canopies. However, according to our model simulations the effective snow crystal size is much larger that the measured mean snow crystal size. The models are used to analyze the effect of various snow parameters to C-band backscattering and to define the accuracy of two snow melt radar algorithms.*

# 1. INTRODUCTION

Snow cover has a substantial impact on processes regarding the interaction between the atmosphere and surface; thus, the knowledge of snow parameters is important for climatology, meteorology, flood prevention and hydropower industry. The applicability of remote sensing for snow monitoring and has been investigated for years. Remote sensing instruments offer a method for monitoring the snow cover, as successfully demonstrated in [1], [2], [3], [4], [5] and [6]. Remote sensing provides logistical advantages compared with gauging networks. Radar measurements are independent of light and weather conditions and the data are available worldwide. This is particularly important in remote areas, where gauging networks are sparse or non-existent [7].

However, few studies have analyzed the effect of various snow characteristics to the accuracy of SAR-based snow extent estimation during the melting season. Previous studies have mainly shown results obtained by comparing SAR-derived snow extent estimates with ground surveys or satellite-borne optical images [3], [4], [6], [8]. This paper presents a simple snow backscattering model combined with the HUT semi-empirical forest backscattering model. The model is validated with HUTSCAT scatterometer and ERS-1 SAR data acquired in the Sodankylä test site. The model is used to analyze the effect of several parameters affecting the accuracy of snow extent monitoring by radar is analyzed.

# 2. TEST SITE AND DATA

Our test site is located in Sodankylä in northern Finland (center latitude = 67.41 N, center longitude = 26.58 E) and its size is 40 km by 40 km. A total of 19 test lines was selected within the test site for airborne and ground-based measurements [9]. The total length of the test lines is over 9 km. The properties of the forest canopies along the test lines were measured, including the tree type, height and stem volume. Extensive field measurements were conducted along the test lines during the airborne campaigns [9]. The measured parameters include the snow extent, physical parameters of snow cover and underlying soil and, additionally, weather data [9]. In this study we use HUTSCAT ranging scatterometer data and ERS-1 SAR data collected on May 1, 1992 and January 20, 1993 [9]. The *in situ* data and the selection of remotely sensed data is more thoroughly explained in [9]. The summary of the *in situ* data is listed in Table 1.

***Table 1.*** *Observed weather and soil conditions in the Sodankylä test site.*

| Date | Air temperature (°C) | Test line (land cover) | Snow depth (cm) | Snow density (g/cm³) | Snow wetness (%) | Crystal size (mm) |
|---|---|---|---|---|---|---|
| May 1, 1992 | 1.3 to 8.4 | clear-cut | 58 | 0.31 | 2.0 | 0.5-3.0 |
| | | pine 0-50 m³/ha | 60 | 0.27 | 2.5 | |
| | | pine 50-100 m³/ha | 60 | 0.27 | 2.7 | |
| | | pine 100-150 m³/ha | 57 | 0.26 | 2.9 | |
| | | open bog | 40 | 0.32 | 5.3 | |
| | | mire | 66 | 0.26 | 2.9 | |
| | | gravel | 38 | 0.28 | 4.0 | |
| | | field | 47 | 0.30 | N/A | |
| January 20, 1993 | -8.0 to –24.2 | clear-cut | 75 | 0.20 | 0 | 0.5-2.7 |
| | | pine 0-50 m³/ha | 72 | 0.20 | 0 | |
| | | pine50-100 m³/ha | 76 | 0.20 | 0 | |
| | | pine 100-150 m³/ha | 73 | 0.20 | 0 | |
| | | open bog | 48 | 0.22 | 0 | |
| | | mire | 83 | 0.20 | 0 | |
| | | gravel | 60 | 0.22 | 0 | |
| | | field | 74 | 0.21 | 0 | |

# 3.  THE MODELING APPROACH

## 3.1  The backscattering model

In general, the backscattering coefficient of snow-covered terrain may consist of direct contributions resulting from [10], [11]:

A)  backscattering from the snow-air interface,

B)  volume scattering from the snow layer,

C)  backscattering from the underlying ground surface and

D)  indirect contributions resulting from wave interaction between volume inhomogeneities and the snow-ground interface.

Backscattering contributions A, B and C are illustrated in Figure 1. The snow-covered terrain is considered as an inhomogeneous layer above a homogeneous half space.
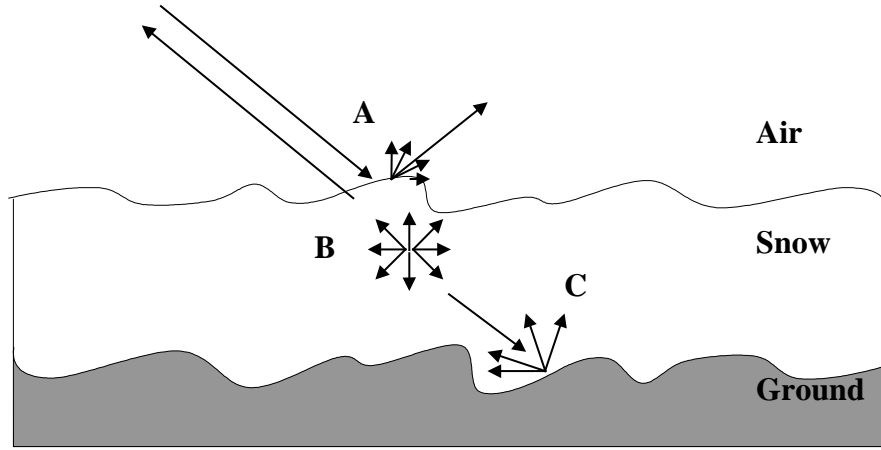
*Figure 1.* The scattering mechanisms of snow-covered terrain: A) backscattering from the snow-air interface, B) volume scattering from the snow layer and C) backscattering from the underlying ground surface.

The total backscattering is the sum of components A to D mentioned above. However, the magnitude of component D is much smaller than the others and, therefore, it can be neglected [11]:

$$\sigma^0 = \sigma_A^0 + \sigma_B^0 + \sigma_C^0 \quad . \tag{1}$$

This model is based on two main assumptions [10]:

1. Only single scattering is important.

2. The transmission through the upper boundary can be modeled using the Fresnel power transmission coefficient.

The observed backscattering coefficient is affected by several physical parameters of the snow layer. These parameters are [10], [11], [12]:

- volumetric liquid water content,

- snowpack depth,

- surface roughness (air-snow boundary and snow-ground boundary),

- snow crystal size (grain size) and shape,

- snowpack density profile,

- layering.

An often employed snowpack characteristic is the snow water equivalent (SWE) which is directly related to the snowpack depth and density. In addition to the

characteristics mentioned above, information on vegetation characteristics (forest canopy) is required [13].

### 3.1.1 Upper boundary surface scattering

The upper surface scattering is modeled by using the IEM scattering model [11]. The general form of the model is following:

$$\sigma_A^0 = 4\pi \cos\theta_s \left[ I_v(\mu_s, \phi_s) / I_v^i \right] \Big|_{\theta_s = \theta} =$$

(2)

$$\frac{k^2}{2} \exp\left(-2k_z^2\sigma^2\right) \sum_{n=1}^{\infty} \left|I_{vv}^n\right|^2 \frac{W^n(-2k_x, 0)}{n!}$$

where

$$I_{vv}^n = (2k_z\sigma_s)^n f_{vv} \exp\left(-2k_z^2\sigma_s^2\right) + \frac{(k_z\sigma_s)\left[F_{vv}(-k_x, 0) + F_{vv}(k_x, 0)\right]}{2}.$$

(3)

In Equations (2) and (3) $\theta$ is the incidence angle, $\sigma_s$ is the snow surface rms-height, $k = 2\pi / \lambda$, $\lambda$ is the wavelength in air, $k_x = k \cos\theta$ and $k_z = k \sin\theta$. The term W represents the correlation function. In this model the exponential correlation function is applied [11].

For the monostatic case the equations for $f_{vv}$, $F_{vv}(k_x, 0)$ and $F_{vv}(-k_x, 0)$ can be found in [11]. These parameters are related to the dielectric properties of snow. The complex dielectric constant of snow is obtained from the modified Debye-like formula introduced in [14].

### 3.1.2 Volume scattering and total attenuation in snowpack

For the volume scattering contribution a simple model using a plane interface is employed [11]:

$$\sigma_B^0 = 0.5\omega * T_{lt}T_{tl} \cos\theta \left[ 1 - \exp\left(-\frac{2\tau}{\cos\theta_t}\right) \right] P_{vv}(\cos\theta_t, -\cos\theta_t; \pi),$$

(4)

where $T_{ij}$ is the Fresnel power transmission coefficient from medium j to i. $P_{vv}$ is the phase function for volume scattering and $\tau = \kappa_e * d_s$ (snow depth) [11].

The albedo ($\omega$) of the medium is the relation of $\kappa_s/\kappa_e$, where $\kappa_s$ is $\kappa_e = \kappa_s + \kappa_a$. $\kappa_s$ can be calculated using the theoretical Rayleigh scattering approximation [10]. For the volume fraction a value 0.6 is applied [15].

The absorption coefficient ($\kappa_a$) is approximated using $\kappa_a = 2k \cdot im\left|\sqrt{\varepsilon_S}\right|$.

### 3.1.3 Lower boundary surface scattering

The noncoherent scattering contribution attenuated by the snow medium, can be estimated by applying the following formula [11]:

$$\sigma^0{}_C = \cos(\theta) T_{lt}(\theta,\theta_t) T_{tl}(\theta_t,\theta) \exp\left(-\frac{2\tau}{\cos\theta_t}\right) \frac{\sigma^0{}_{gr}(\theta_t)}{\cos(\theta_t)} , \qquad (5)$$

In Equation (5) $\sigma^0{}_{gr}$ is the surface scattering term for the lower boundary. It is approximated using the Michigan empirical surface scattering model [16].

$$\sigma^0_{gr} = \frac{g \cdot \cos^3\theta_t}{\sqrt{p}} \cdot [\Gamma_v(\theta_t) + \Gamma_h(\theta_t)] , \qquad (6)$$

Where

$$\sqrt{p} = 1 - \left(\frac{2\theta_t}{\pi}\right)^{\left[\frac{1}{3\Gamma_0}\right]} \cdot \exp(-k_s\sigma_g) \qquad (7)$$

$$g = 0.7\left[1 - \exp\left(-0.65 \cdot (k_s\sigma_g)^{1.8}\right)\right] . \qquad (8)$$

The Fresnel reflectivity of the surface at nadir $\Gamma_0 = \left|\frac{1-\sqrt{\varepsilon_r}}{1+\sqrt{\varepsilon_r}}\right|^2$ where $\varepsilon_r = \frac{\varepsilon_g}{\varepsilon_s}$. The

wave number in the snow is denoted $k_s$ and $\sigma_g$ is the ground surface rms-height.

Figure 2 shows the behavior of various backscattering contributions as a function of snow wetness using the backscattering model introduced above. In the simulation the snow surface correlation length is 5.0 cm, the rms-height is 0.4 cm; the frozen ground permittivity is 6-j and the ground rms-height is 1.2 cm. Based on experimental data, the frozen ground permittivity of 6-1j is a realistic value as frozen soil can include some liquid water even at soil temperatures as low as -24 $^o$C [17]. The snow crystal size represents the effective snow crystal size. It has been previously reported that when discrete particle backscattering model is used at C-band, the effective crystal size is larger than the observed mean crystal size [18], [19]. In this case the behavior of the target cannot be explained in terms of the particles of which the snowpack was observed. The particles must be considered as "sticky" particles, where the particles come together to form an aggregate particle, effectively much larger than the individual particles [20]. The authors in [18] found that the effective crystal size was six times larger than the observed mean crystal size at C-band.

From Figure 2 it can be seen that the volume scattering dominates up to 4% of volumetric wetness and surface scattering dominates at higher wetnesses. In the dry snow case (snow layer depth=100 cm) the scattering contribution coming from the

ground layer has an almost negligible effect to the total backscattering coefficient due to the high amount of volume scattering.
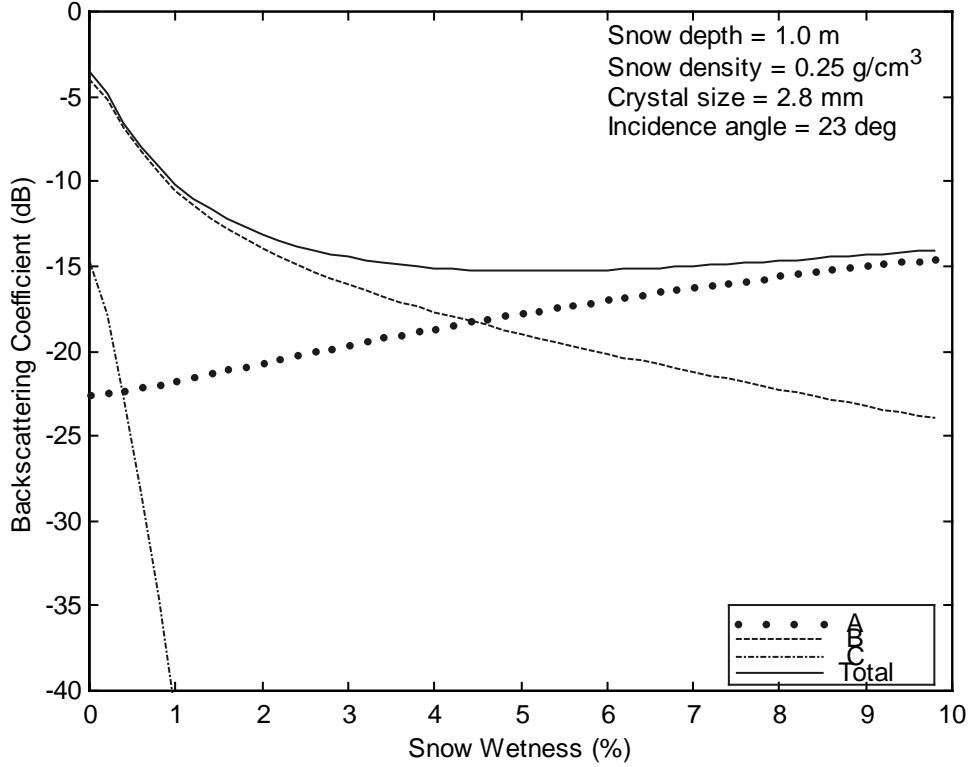


*Figure 2. Modeled backscattering contributions A, B and C as a function of snow wetness. The snow surface correlation length is 5.0 cm, rms-height is 0.4 cm; the frozen ground permittivity is 6-j and soil surface rms-height is 1.2 cm.*

# 4. EFFECT OF FOREST CANOPY BASED ON EXPERIMENTAL DATA AND MODELING

The spatially varying forest cover causes additional problems for radar monitoring of snow cover. The forest canopy backscatters the radar signal and, on the other hand, attenuates the signal contribution backscattered from the snow-covered terrain. A quantitative investigation on the effect of forest canopy is accomplished in this paper by applying the previously developed semi-empirical boreal forest backscattering model [20], [21], [22], [23] together with radar observations. The radar data include HUTSCAT ranging scatterometer and ERS-1 SAR observations of the Sodankylä test site, northern Finland [9].

The backscattering contributions of forest canopy and forest floor can be directly distinguished from HUTSCAT ranging scatterometer data. As the semi-empirical forest backscattering model is fitted into HUTSCAT observations for a forested test

site, the average behavior of forest canopy and forest floor backscatter as a function of stem volume is obtained. Obviously, this requires experimental data representing various stem volume classes. The backscattering coefficient $\sigma°$ of forested terrain measured by a SAR can be given as a sum of forest floor and forest canopy backscattering contributions, $\sigma°_{floor}$ and $\sigma°_{can}$, respectively:

$$\sigma_{forested\_terrain}{}^{o}(V,\theta,m_{v,can},\sigma_{terrain}^{o}) = \sigma_{can}^{o} + \sigma_{floor}^{o}$$

(9)

$$\equiv \sigma_{can}^{o}(V,\theta,m_{v,can}) + t^{2}(V,\theta,m_{v,can}) \cdot \sigma_{terrain}^{o}$$

where

| | | |
|---|---|---|
| V | = | forest stem volume, |
| $\theta$ | = | angle of incidence, |
| $m_{v,can}$ | = | effective vegetation (forest canopy) moisture level / frost status (related to the effective permittivity of forest canopy), |
| $\sigma°_{terrain}$ | = | backscattering coefficient of snow-covered terrain and |
| $t^{2}$ | = | two-way forest canopy transmissivity. |

Equations for relating $\sigma°_{can}$ and $t^{2}$ with V, $\theta$ and $m_{v,can}$ are given in [22].

The influence of forest cover on $\sigma°$ is analyzed here by estimating $\sigma°_{floor}$ and $\sigma°_{can}$ from HUTSCAT experiments representing (a) dry snow and (b) wet snow conditions. Figure 3 depicts the behavior of $\sigma°$, $\sigma°_{floor}$ and $\sigma°_{can}$ as estimated by fitting the semi-empirical model into HUTSCAT observations ($m_{v,can}$ and $\sigma°_{terrain}$ as optimized parameters) . The dry snow observations were conducted during a long cold mid-winter period on 20 January 1993 (air temperature variation from –24.2 to –8.0°C on 20 January). The wet snow measurements were carried out during a spring melt period on 1 May 1992 (air temperature variation from 1.3 to 4.5°C on 1 May). Hence, the forest canopy was frozen in January and thawed in May. Experimental investigations indicate that the freezing of trees rapidly starts at the temperatures from –5°C to –7°C [24], [25].
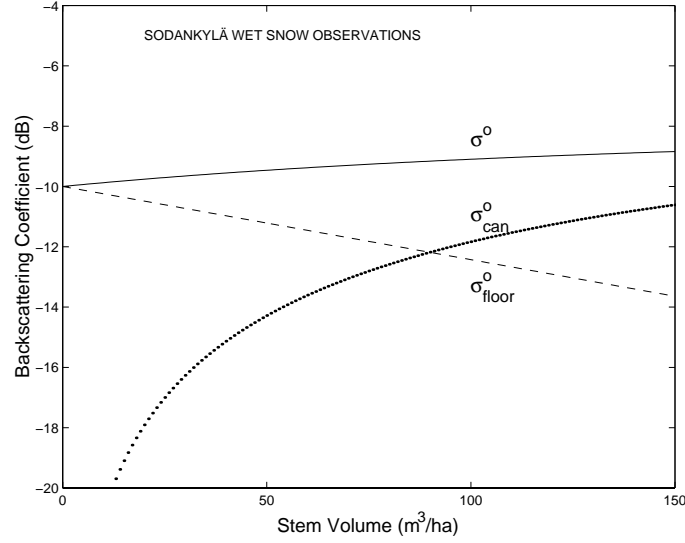
(a)



10
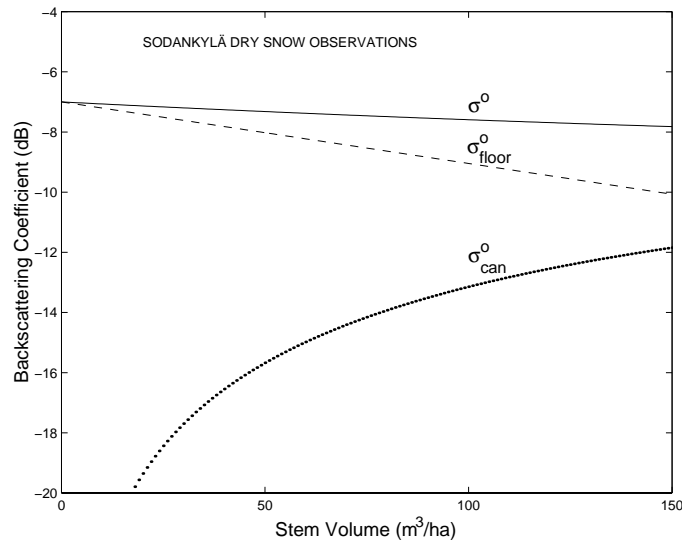
(b)



**Figure 3**. *C-band backscattering contributions,* $\sigma^c_{forested\_terrain}$, $\sigma^o_{floor}$ *and* $\sigma^o_{can}$ *in (9), under (a) dry snow conditions and (b) wet snow conditions. The modeled response of* $\sigma^o_{floor}$ *and* $\sigma^o_{can}$ *to stem volume is based on HUTSCAT observations conducted on 20 January 1993 (dry snow and frozen forest canopy) and 1 May 1992 (wet snow and thawed forest canopy). The incidence angle is 23$^c$ and polarization VV corresponding to ERS-1/2 SAR observations.*

In Figure 4, the level of snow-covered terrain backscatter $\sigma^o_{terrain}$ (equal to $\sigma^o$ in Equation 1 for V = 0 m$^3$/ha) is determined according to ERS-1 SAR observations of deforested areas. The SAR imaging was conducted simultaneously with HUTSCAT measurements. However, $\sigma^o_{terrain}$ may vary significantly according to snow cover characteristics. Therefore, Figure 4 depicts the behavior of $\sigma^o_{forested\_terrain}$ as a function of stem volume with various $\sigma^o_{terrain}$ level as a parameter. The four top-most curves represent typical dry snow conditions, when the effect of forest canopy is considered with model parameters corresponding to mid-winter observations and $\sigma^o_{terrain}$ varies within a typical range corresponding to various dry snow conditions. The model parameters are estimated identically to Figure 3(a) from HUTSCAT measurements conducted on 20 January 1993. The three lowest curves in Figure 3(b) represent typical wet snow conditions and $\sigma^o_{terrain}$ varies within a typical range corresponding to various wet snow conditions. In that case, the forest canopy effects are considered according to HUTSCAT observations of 1 May 1992, identically to Figure 3(b). As the dry snow HUTSCAT measurements represent very cold conditions, the correlation of $\sigma^o$ with stem volume is negative for curves representing the dry snow case. The correlation may turn positive if the temperature is only slightly below 0°C. Under that kind of conditions the forest canopy is typically partially thawed, which causes a higher level of $\sigma^o_{can}$.

The results in Figures 3 and 4 indicate that the effect of forest cover on $\sigma^o$ is relatively small compared with that of snow cover characteristics, especially snow wetness.

11

However, as Figure 4 depicts, the spatially varying forest cover (stem volume) may cause major difficulties for snow mapping algorithms as the difference in $\sigma^{\circ}_{forested\_terrain}$ between dry and wet snow cases is strongly dependent on forest stem volume.
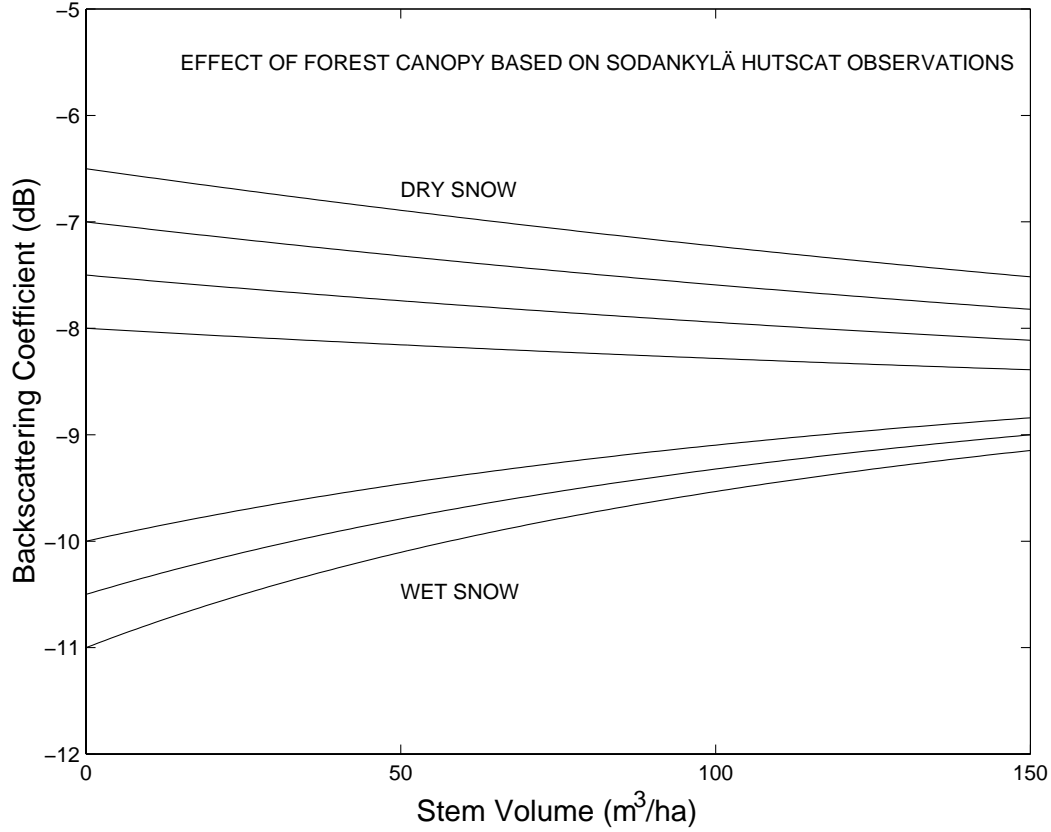


EFFECT OF FOREST CANOPY BASED ON SODANKYLÄ HUTSCAT OBSERVATIONS

DRY SNOW

WET SNOW

**Figure 4.** Modeled response of C-band $\sigma^{\circ}$ to forest stem volume (biomass) under typical dry snow and frozen canopy condition (four top curves) and wet snow and thawed canopy conditions (three lowest curves). $\sigma^{\circ}_{forested\_terrain}$ is calculated by (9) employing the forest canopy transmissivity $t^2$ and canopy backscattering coefficient $\sigma^{o}_{can}$ determined as in Figure 3 from HUTSCAT observations. Incidence angle is 23° and polarization VV.

# 5. VERIFICATION OF THE MODEL

The model predictions were compared with HUTSCAT and ERS-1 SAR data for the Sodankylä test site. The ground truth was collected from every test line, however, the ground truth observations of the snow crystal size were carried out in one sample plot. The observed crystal size varied from 0.5 to 3.0 mm with an average size less than 1 mm. The snow wetness did not have a large effect to the crystal size; however, the shapes of wet snow crystals were nearly spherical. As was mentioned earlier when the discrete particle backscattering model is used at C-band, the effective crystal size is

larger than the observed mean crystal size. Therefore, the model was fitted with the radar data by simulating crystal size as a free parameter. Figure 5 depicts the best results of the comparison. Figure 5 shows results from calculation with two crystal sizes, 2.8 mm and 3.2 mm. For forested terrain the backscattering contribution from the canopy was calculated using the model introduced in Section 4. The results show clearly that our model predictions agree reasonably well with the behavior of ERS and HUTSCAT observations. In the case of dry snow, we can see the slightly negative trend as a function of stem volume while in the case of wet snow the behavior is reversed. The open bog was considered as open area and mire as sparsely forested terrain in model simulation. A change in the snow crystal size mainly causes a shift in the level of modeled $\sigma^o$ curve, whereas the shape of the $\sigma^o$ curve remains the same. Our results indicate that the crystal size of 2.8 mm gives the best fit in the dry snow case. However, for the wet snow case the predicted backscattering values tend to be too small. Our observations agree with [18], which suggests that the effective crystal size is much larger at C-band than the observed mean crystal size.
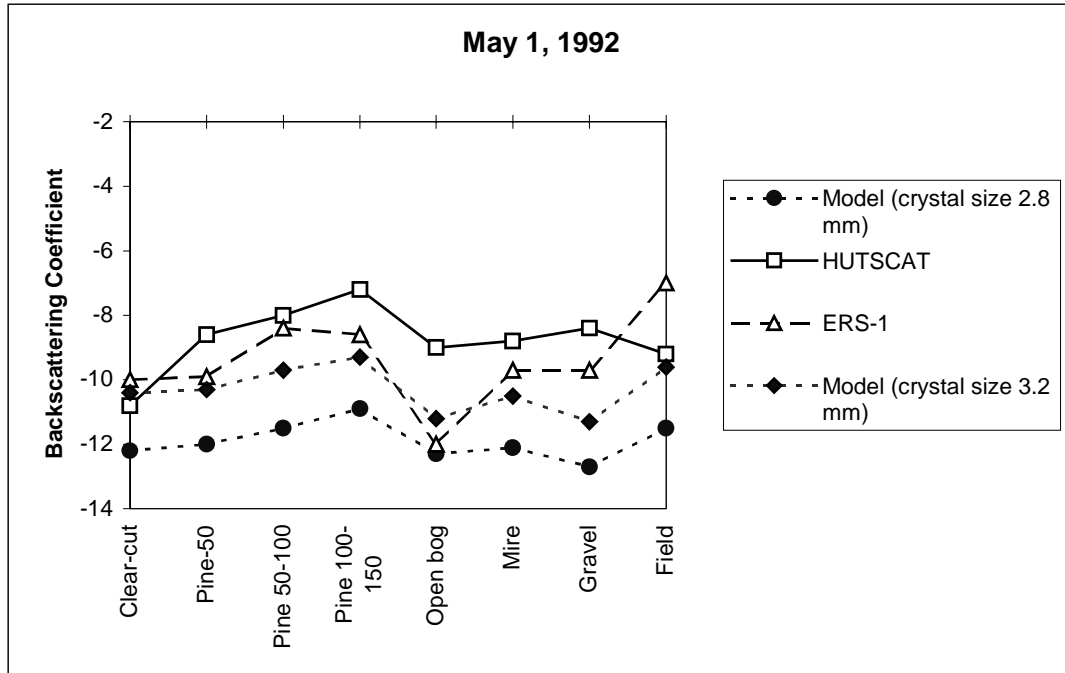
(a)



January 20,1993
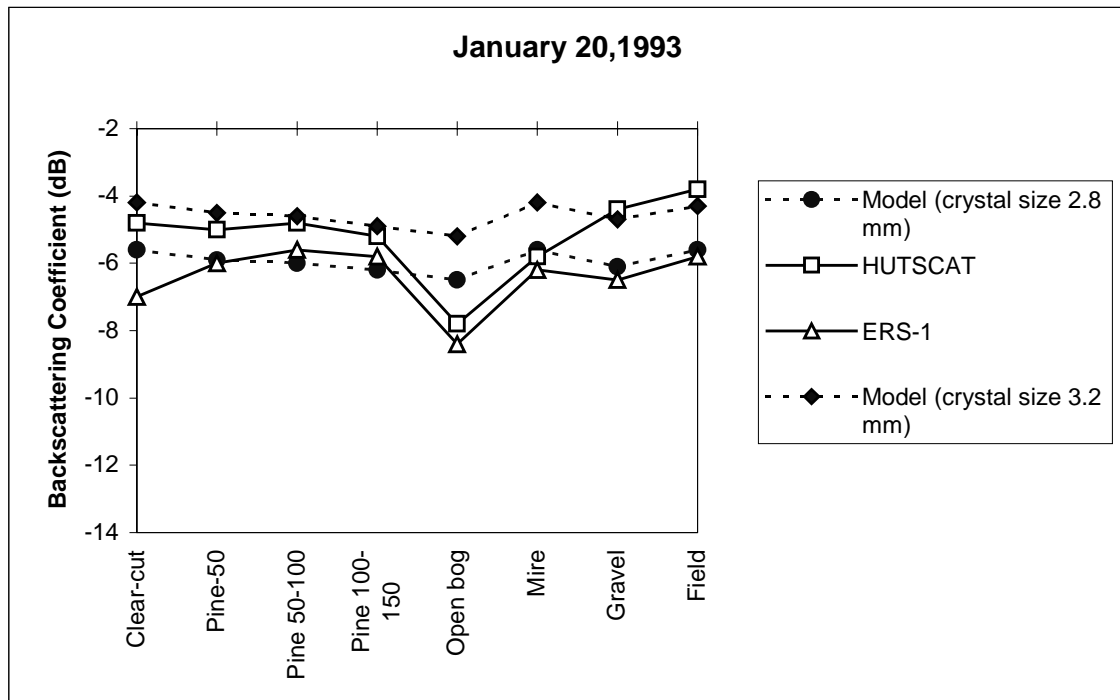
(b)



**Figure 5.** *Comparison of snow and forest model predicted backscattering coefficients with HUTSCAT and ERS-1 derived backscattering coefficients. The snow model employs crystal sizes of 2.8 mm and 3.2 mm and the forest canopy contribution estimation is based on results plotted in Figure 3. The comparison is performed for (a) dry snow conditions and (b) wet snow conditions.*

# 6. EVALUATION OF TWO SNOW EXTENT ALGORITHMS BASED ON THE MODEL

The main principle of the snow melt algorithm developed in HUT [4] is that the fraction of snow cover in every pixel is estimated by comparing a SAR image acquired during the snow melt period with the reference images acquired at the beginning of the snow melt period (the whole area is covered by wet snow) and after the snow melt period (the whole area is free of snow and the ground is wet). Since this algorithm applies pixel-wise comparison of SAR images, which are rectified using a DEM, the surface roughness and slope of the soil and forest stem volume are constant in every pixel for the three SAR images.

Another snow melt algorithm approach is to compare a SAR image acquired during the snow melt period with a dry snow reference image [6]. By applying the model presented in Section 3 we can investigate the effect of various snow parameters to the total backscattering from snow-covered terrain as a function of snow wetness. This information can be used to compare the accuracy characteristics of the two snow melt algorithms mentioned above. Figure 6 shows the modeled ratio of (a) $\sigma^o$ for dry snow and $\sigma^o$ for wet snow and (b) $\sigma^o$ for snow-free ground and $\sigma^o$ for wet snow with various

14

physical snow and soil characteristics for non-forested terrain. For forested terrain the backscattering ratio gets smaller as the stem volume and canopy moisture increases. In both cases presented in Figure 6 (a) and (b) we have used following ranges of variation:

- snow depth: 20 to 200 cm,

- snow density: 0.2 to 0.5 g/cm$^3$,

- effective snow crystal size: 2 to 4 mm.

- snow surface roughness: rms 0.4 cm , correlation length 5.0 cm

- ground surface roughness: rms 1.2 cm.

The variation ranges are selected to represent the typical cases in Finland. However, both snow and ground surface roughness characteristics represent the average values reported in the literature [11], [18], [26] and snow crystal size represents the effective snow crystal size [18]. In the HUT snow melt algorithm the snow-free ground moisture is assumed to randomly vary from 25 to 30%. The results are presented as a function of snow wetness. In the Figures 6 (a) and (b) vertical bars indicate the standard deviation.

Figure 6 (a) presents the results from dry snow vs. wet snow algorithm (dry snow reference). Our calculations show that the standard deviation of the backscattering coefficient difference is more than 2 dB for every snow wetness class due to the assumed changes in the dry snow and wet snow images. Most of the variation is due to the variation of volume scattering in the snow layer. For thin snow layers (0.5 m) the effect of ground scattering dominates and, therefore, the total backscattering is lower than that for thicker snow layers where the volume effect dominates. Also in this algorithm the snow crystal size varies for both wet and dry snow, which increases the standard deviation. The best results are obtained when the dry snow layer is more than 1 m thick and the wet snow wetness is above 2 %.

The model simulations depicted in Figure 6 (b) show that the average behavior of the HUT snow melt algorithm is similar to that in Figure 6(a); however, the standard deviation of HUT algorithm is smaller. The HUT algorithm gives most accurate estimates when the snow wetness is above 2 %. In this case the standard deviation of the difference is less than 2 dB (the mean difference varies from 6.5 to 7.4 dB). In principle the level of backscattering from snow-free ground in the HUT algorithm also depends on the surface roughness, but since the comparison is always done pixel-wise this effect can be eliminated.
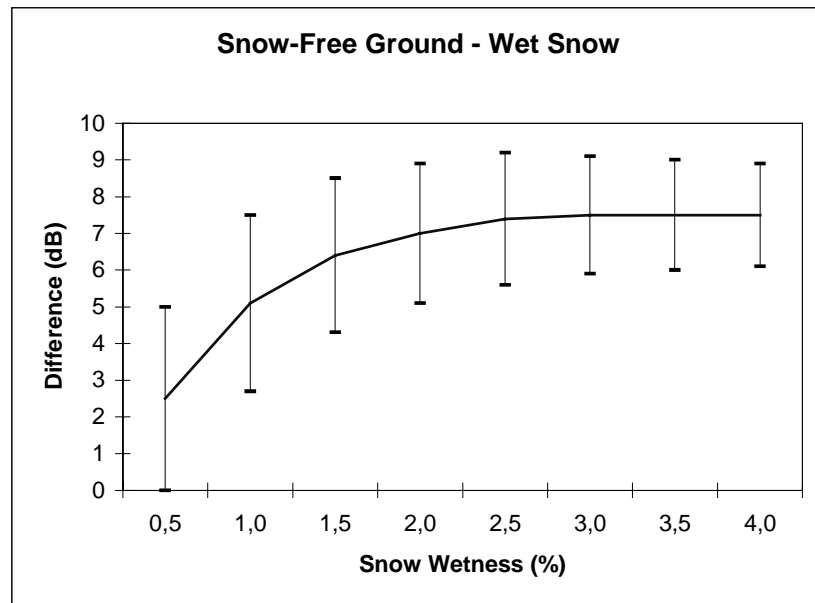
(a)
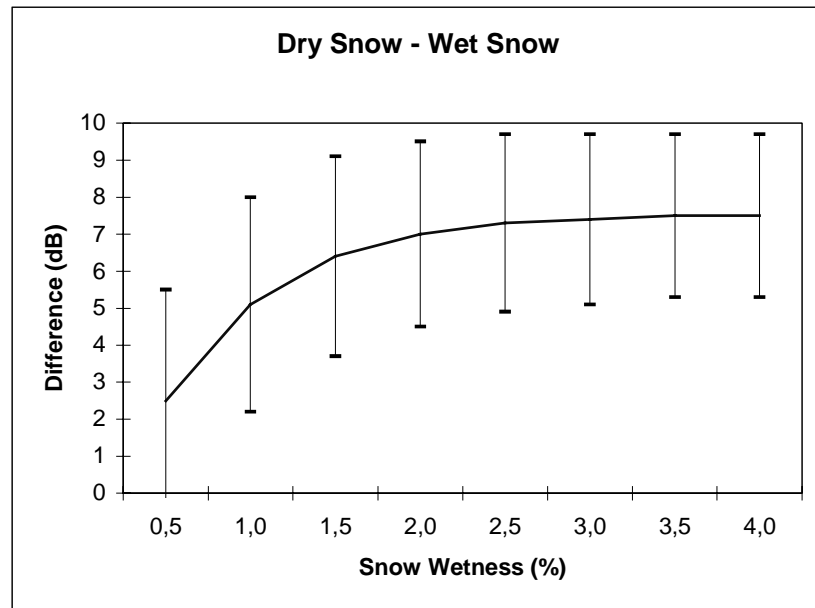


(b)



*Figure 6. Modeled behavior of backscattering coefficient difference between (a) dry snow and wet snow and (b) wet snow and snow-free ground as a function of snow wetness. The calculation is based on various snow depths (20-200 cm), snow densities (0.2-0.5 g/cm³) and effective snow crystal sizes (2.0-4.0 mm). The vertical bars indicate the standard deviation of the mean backscattering differences.*

# 7. CONCLUSIONS

The possibility to use C-band microwave radar in snow monitoring has been studied intensively during the past few last years and promising results have been obtained detecting and monitoring snow melt. However, no theoretical considerations concerning the effect of various snow parameters to the accuracy of these monitoring systems have been presented. We have described a simple backscattering model for snow monitoring in forested areas. The backscattering model is very general and as mentioned earlier it does not consider multiple scattering. Therefore, it does not fully describe all aspects of backscattering from snow-covered ground. The model simulations describe the behavior of snow cover in boreal forest and, therefore, may not correspond to the snow conditions in mountainous areas. The model has been verified with our previous measurements in the Sodankylä test site and its predictions agree reasonably well with the data. By using the backscattering model we have investigated the effect of various snow parameters to the backscattering coefficient. These simulations have been used to follow how much various parameters affect the SAR-based snow extent monitoring systems, where the difference between dry snow and wet snow or wet snow and snow-free ground is observed. Our results show that

- a simple backscattering model is sufficient to simulate the general behavior of backscattering from snow-covered terrain,

- by using a semi-empirical boreal forest backscattering model information from the snow layer can be obtained even in the presence of forest canopies, and

- the snow melt monitoring approaches employing the backscatter difference between wet snow and snow-free ground give more accurate results than the techniques employing the difference between dry and wet snow. The best result is obtained when the snow wetness is higher than 2%.

# 8. REFERENCES

[1]  R. Kuittinen, "Remote sensing for hydrology progress and prospects", *WMO Operational Hydrology report*, No. 36, WMO-No. 773, Geneva-Switzerland, 1992.

[2]  R. Solberg and T. Andersen, "An automatic system for operational snow-cover monitoring in the Norwegian mountain regions*," Proceedings of IEEE International Geoscience and Remote Sensing Symposium (IGARSS'94)*, Pasadena, California, USA, pp. 2084-2086, 1994.

[3]  J. Piesbergen, F. Holecz and H. Haefner, "Snow cover monitoring using multitemporal ERS-1 SAR data", *Proceedings of IEEE International Geoscience and Remote Sensing Symposium (IGARSS'95)*, Florence, Italy, pp. 1750-1752, 1995.

[4]  J. Koskinen, J. Pulliainen and M. Hallikainen, "The use of ERS-1 SAR data in snow melt monitoring", *IEEE Trans. on Geoscience and Remote Sensing*, Vol. 35, No. 3, pp. 601- 610, 1996.

[5]  T. Guneriussen, "Backscattering properties of a wet snow cover derived from DEM corrected ERS-1 SAR data", *Int. J. Remote Sensing*, Vol. 18, No. 2, pp. 375-392, 1997.

[6]  T. Nagler and H. Rott, "SAR tools for snowmelt modeling in the project HydAlp", *Proceedings of IEEE International Geoscience and Remote Sensing Symposium (IGARSS'98) Symposium*, Seattle, USA, 1998.

[7]  R. Solberg, D. Hiltbrunner, J. Koskinen, T. Gunneriussen, K. Rautiainen and M. Hallikainen, "Snow algorithms and products", Report from SNOWTOOLS WP410, Norwegian Computing Center, *Report 924*, Norway, 112 p., 1997.

[8]  J. Koskinen, S. Metsämäki, J. Grandell, S. Jänne, L. Matikainen, M. Hallikainen, "Snow monitoring using radar and optical satellite data", *Remote Sensing of Environment*, Vol. 69, No. 1, pp. 16-29, 1999.

[9]  J. Koskinen, J. Pulliainen, M. Mäkynen, and M. Hallikainen, "Seasonal comparison of HUTSCAT ranging scatterometer and ERS-1 SAR microwave signatures of boreal forest zone", *IEEE Trans. Geoscience and Remote Sensing*, Vol. 37, No. 4, pp. 2068-2080, 1999.

[10] F. Ulaby, R. Moore and A. Fung, "Microwave remote sensing, active and passive", *Volume III. Reading, Addison Wesley*, 1986.

[11] A. Fung, "Microwave scattering and emission models and their applications", *Artech House*, 573 p. 1994.

[12] J. Pulliainen, P. Mikkelä, M. Hallikainen and J-P. Ikonen, "Seasonal dynamics of C-Band backscatter of boreal forests with application to biomass and soil moisture estimation", *IEEE Trans. Geoscience and Remote Sensing*, Vol. 34, No. 3, pp. 758-770, 1996.

[13] J. Pulliainen, J. Grandell, M. Hallikainen, M. Virtanen, N. Walker, S. Metsämäki, J. Ikonen, Y. Sucksdorf and T. Manninen, "Scatterometer and radiometer land applications", Final Report, *ESRIN Contract No: 11122/94/I-HE(SC),* 255 p., 1996.

[14] M. Hallikainen, F. Ulaby and M. Abdelrazik, "Dielectric properties of snow in the 3-37 GHz range", *IEEE Trans. Antennas and Propagation*, Vol. 34, No. 11, pp. 1329-1340, 1986.

[15] T. Guneriussen, "Backscattering properties of a wet snow cover derived from DEM corrected ERS-1 SAR data", *International Journal of Remote Sensing*, Vol. 18, No. 2, pp. 375-392, 1997.

[16] Y. Oh, K. Sarabandi and F. Ulaby, "An empirical model and an inversion technique for radar scattering from bare soil surfaces", *IEEE Trans. Geoscience and Remote Sensing*, Vol. 30, No. 2, pp. 370-381, 1992.

[17] M. Hallikainen, F. Ulaby, M. Dobson, M. El-Rayes and L.-K. Wu, "Microwave dielectric behavior of wet soil - Part I: Empirical models and experimental observations," *IEEE Trans. Geoscience and Remote Sensing*, Vol. 23, pp. 25-34, 1985.

[18] J. Kendra, K. Sarabandi and F. Ulaby, "Radar measurements of snow: experiments and analysis", *IEEE Trans. Geoscience and Remote Sensing*, Vol. 36, No. 3, pp. 864-879, 1999.

[19] L. Zurk, K. Ding, L. Tsang and D. Winebrenner, "Monte Carlo Simulations of the Extinction Rate of Densely Packed Spheres with Clustered and Nonclustered geometries, *Proceedings of IEEE International Geoscience and Remote Sensing Symposium (IGARSS'94) Symposium,* Pasadena, USA, 1994.

[20] J. Pulliainen, "Investigation on the backscattering properties of Finnish boreal forests at C- and X-band: A semi-empirical modeling approach," Doctoral dissertation, Laboratory of Space Technology, Helsinki University Technology, Report 19, 1994.

[21] J. Pulliainen, K. Heiska, J. Hyyppä, and M. Hallikainen, "Backscattering properties of boreal forests at the C- and X-bands," *IEEE Trans. Geosci. Remote Sensing*, Vol. 32, pp. 1041-1050, 1994.

[22] J. Pulliainen, L. Kurvonen, and M. Hallikainen, "Multi-temporal behavior of L- and C-band SAR observations of boreal forests", *IEEE Trans. Geoscience and Remote Sensing*, Vol. 37, pp. 927-937, 1999.

[23] J. Pulliainen, K. Heiska, J. Hyyppä, and M. Hallikainen, "Backscattering properties of boreal forests at the C- and X-bands", *IEEE Trans. Geoscience and Remote Sensing*, Vol. 32, pp. 1041-1050, 1994.

[24] M. Kärkkäinen, "Tree Science", *Karisto,* (in Finnish), Helsinki, Finland. pp. 241-267, 1985.

[25] R. Lin, "Review of the electrical properties of wood and cellulose," *Forest Products Journal,* Vol. 17, pp. 54-61, 1967.

[26] J. Shi and J. Dozier, "Inferring snow wetness using C-band data from SIR-C's polarimetric synthetic aperture radar" *IEEE Trans. Geoscience and Remote Sensing,* Vol. 33, No. 4, pp. 905-914, 1995.